A Cooperative Protocol for Vehicle Merging Using Bi-dimensional Artificial Potential Fields

Liu, Zhengqiang; Liu, Di; Yu, Wenwu; Baldi, Simone

Citation (APA)
Liu, Z., Liu, D., Yu, W., & Baldi, S. (2022). A Cooperative Protocol for Vehicle Merging Using Bi-dimensional Artificial Potential Fields. In J. Kim, B. Englot, H.-W. Park, H.-L. Choi, H. Myung, J. Kim, & J.-H. Kim (Eds.), *Robot Intelligence Technology and Applications 6 : Results from the 9th International Conference on Robot Intelligence Technology and Applications* (pp. 566-577). (Lecture Notes in Networks and Systems; Vol. 429 LNNS). Springer. https://doi.org/10.1007/978-3-030-97672-9_51

Important note
To cite this publication, please use the final published version (if applicable).
Please check the document version above.

A Cooperative Protocol for Vehicle Merging Using Bi-dimensional Artificial Potential Fields

Zhengqiang Liu[1], Di Liu[1,4], Wenwu Yu[2,1], and Simone Baldi[2,1,3]

[1] School of Cyber Science and Engineering, Southeast University, Nanjing, China,
`18867104077@163.com, liud923@126.com`
[2] School of Mathematics, Southeast University, Nanjing, China,
`wwyu@seu.edu.cn, s.baldi@tudelft.nl`
[3] Delft Center for Systems and Control, TU Delft, The Netherlands
[4] Bernoulli Institute for Mathematics, Computer Science and Artificial Intelligence,
University of Groningen, Groningen 9747AG, The Netherlands

Abstract. In recent years, platooning solutions like cooperative adaptive cruise control (CACC) have been deeply studied. It is common in such platooning literature to assume that the vehicles drive on the same lane (longitudinal platooning). At the same time, lateral control during merging maneuvers is commonly addressed as a path planning problem, in which the ego vehicle changes the lane during merging without necessarily cooperating with its neighboring vehicles (i.e. without considering gap closing). The primary objective of this article is to develop a control strategy which involves both longitudinal and lateral vehicle dynamics, where the vehicles merge and form a platoon in a cooperative way without a priori path planning. Appropriately designed bi-dimensional artificial potential fields are used to achieve this goal and the proposed protocol is verified through simulations with CarSim.

Keywords: Merging maneuver, artificial potential fields, platooning, longitudinal control, lateral control

1 Introduction

Automated vehicles have been a popular research topic over the last decades [1]. Platooning of connected and automated vehicles is regarded as a possible solution to future transportation, with improved throughput and safety [2–4]. Adaptive cruise control (ACC) system was one of the first technologies to achieve platooning to some extent, and cooperative adaptive cruise control (CACC) is its extension. In CACC, vehicles gather information transmitted from other vehicles via vehicle-to-vehicle (V2V) communication [5–7].

Many different CACC protocols have been proposed to address different requirements. Optimization-based CACC solutions typically rely on model predictive control [8]. The theory of Artificial Potential Fields (APF) is also widely used in CACC. APF can be thought as a virtual energy field that is designed to

---

Corresponding authors: Wenwu Yu and Simone Baldi

achieve certain objectives such as gap-closing and collision avoidance. The CACC protocol is designed based on the gradient of the APF, so as to minimize the virtual energy [9,10]. Recently, some CACC protocols based on adaptive control have also been proposed to address uncertainty in vehicle dynamics [11,12].

However, most CACC works only consider longitudinal dynamics, whereas the lane-changing behavior is one of the most common maneuvers when driving, which involves lateral dynamics as well. The vehicle merging problem in a vehicle platoon indeed involves lane-changing behavior and has also been researched recently. In [13], the merging maneuver is addressed in the presence of uncertain vehicle parameters and a platoon of three vehicles. In [14], an adaptive synchronization protocol with driveline uncertainty is used to describe merging maneuvers. These works only consider the longitudinal aspect of merging, i.e. the gap creating and gap closing. Some existing results consider the merging problem as a path following problem, where vehicles follow an optimal path to merge into another lane. Considered merging scenarios include freeway ramp-merging [15], merging at intersections [16], and merging at roundabouts [17]. The approaches in [18,19] consider lateral behavior via a third-order polynomial to represent the lane-change trajectory, but the ego vehicle changes the lane during merging without cooperating with its neighboring vehicles (i.e. without considering gap closing). In these approaches, the path planning is decided a priori, rather than decided in real-time according to the neighbor position: in this sense, the approach is non-cooperative and does not reflect what human drivers do. Therefore, an integrated approach considering longitudinal, lateral and cooperative aspects of merging is still missing, which motivates this work.

The primary objective of this article is to develop a control strategy which involves the longitudinal and lateral dynamics, whereas all the vehicles form a platoon after the merging process in a cooperative way without a priori path planning. The main contributions of this paper are: designing a simple bi-dimensional APF which greatly reduces the complexity of control laws and the two directions are controlled independently at the same time; validating the proposed protocol in a realistic CarSim environment to assess the robustness and adaptability.

The remainder of this paper is organized as follows. Section 2 introduces the vehicle kinematic model and the merging maneuver is also modeled in this part. The potential functions and controllers are designed in Section 3. Section 4 presents the simulation results. Conclusions are given in Section 5.

2 Vehicle Modeling

This section describes the vehicle kinematic model used for the controller design. The bicycle model in Section 2.1 offers a good balance between realistic vehicle dynamics and design complexity, so it is commonly used in the literature to describe the longitudinal and lateral movement of a vehicle [20,21]. The vehicle merging model is introduced in Section 2.2 which is in line with merging scenarios considered in related works [6,7,10,19].

2.1 Rear Axle Bicycle Model

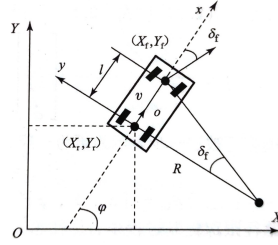A rear axle bicycle model is depicted in Fig. 1.

Fig. 1. Rear axle bicycle model of the vehicle

Let $\varphi[rad]$ be the yaw angle of the vehicle, which is defined as the angle between x-axis and X-axis in Fig. 1. Let (X_r,Y_r) and (X_f,Y_f) be the inertial coordinates of the rear and front axle center of the vehicle, respectively. Let $v[m/s]$ be the velocity of the rear axle center and R the turning radius. Let $\delta_f[rad]$ and $l[m]$ be the front wheel steering angle and the wheelbase, respectively. Because the center of the rear axle is the reference point, (X_r,Y_r) can be used to represent the vehicle's position, i.e. $(X_r, Y_r) = (X, Y)$. The vehicle velocity is:

$$v = \dot{X}_r \cos\varphi + \dot{Y}_r \sin\varphi \tag{1}$$

The following equations describe physical constraints:

$$\dot{X}_f \sin(\varphi + \delta_f) - \dot{Y}_f \cos(\varphi + \delta_f) = 0 \tag{2}$$

$$\dot{X}_r \sin\varphi - \dot{Y}_r \cos\varphi = 0 \tag{3}$$

Using the following relation for the yaw rate $\omega[rad/s]$.

$$\omega = \frac{v}{l} \tan\delta_f \tag{4}$$

and standard geometric relations well described in the literature [1], the following dynamics can be obtained:

$$\begin{bmatrix} \dot{X} \\ \dot{Y} \\ \dot{v} \\ \dot{\varphi} \end{bmatrix} = \begin{bmatrix} v\cos\varphi \\ v\sin\varphi \\ a \\ \omega \end{bmatrix} \tag{5}$$

where the control inputs are the acceleration $a[m/s^2]$ of vehicle and the yaw rate ω.

2.2 Vehicle Merging Model

Vehicles need to merge into another platoon on the adjacent lane if the lane reduction is about to happen, as shown in Fig. 2. In this work we chose the standard merging scenario that was recently proposed in the Grand Cooperative Driving Challenge [6,7,10], in which two platoons formed in different lanes must merge into one lane. It has been shown in [22] that when the merging vehi-
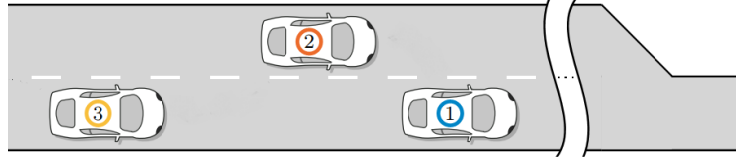

Fig. 2. Three vehicles heading towards a lane reduction (edited from [19]).

cle chooses the adjacent gap as its target, the merging can be broken down into smaller merging sub-problems: in other words, one can consider triplets of vehicles as in [6,7,10], in place of two full platoons. The vehicles in any given triplet will be classified as lead vehicle (vehicle 1 in Fig. 2), merging vehicle (vehicle 2 in Fig. 2) and gap making vehicle (vehicle 3 in Fig. 2), and they are denoted by M_1, M_2, M_3. The lead vehicle is on the lane named lane 1, while the gap making vehicle drives behind the lead vehicle on the same lane. The merging vehicle is on the adjacent lane named lane 2, which will be merging between the lead vehicle and the gap making vehicle. Fig. 3 shows the errors among the various vehicles (for more clarity, only the errors in the longitudinal direction are reported).
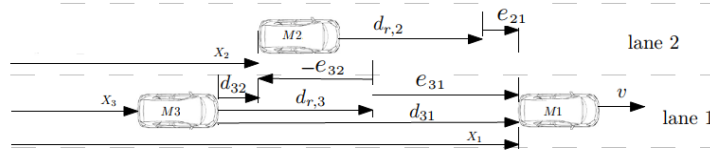

Fig. 3. General triplet for a merging secnario (edited from [10]).

In this merging scenario, the objective is to make gaps between every two vehicles as close as possible to the desired distance $d_{r,i}[m]$ after the merging process to form a new platoon, where

$$d_{r,i}(t) = r_i(t) + hv_i(t), \ i \in S_m \tag{6}$$

where $h[s]$ is the time gap, $r_i[m]$ is the standstill distance which can be made time-varying to the purpose of gap creation, and $S_m = 2, ..., m$ is the set of all following vehicles. This kind of desired distance is called constant time headway, which can meet the requirement of string stability [5, 23].

In the lateral direction of the merging vehicle, a lane change is needed, so the displacement error and yaw angle error of the merging vehicle are required to converge to zero. If $Y_o[m]$ and $\varphi_o[rad]$ are the desired values of lateral displacement and yaw angle, the lateral error variable of interest can be defined as:

$$e_{y_i} = (Y_o - Y_i) + c_1(\varphi_o - \varphi_i) \tag{7}$$

where $Y_i[m]$ is the actual lateral offset, and $\varphi_i[rad]$ is the actual yaw angle for the merging vehicle i. The weight factor of these errors is $c_1[m/rad]$ which is a tuning parameter.

In the longitudinal direction, as Fig. 3 shows, the objective can be described as:

$$\lim_{t \to \infty} e_{21}(t), e_{32}(t) = 0 \tag{8}$$

where

$$e_{21} = d_{21} - d_{r,2} = X_1 - X_2 - L_2 - d_{r,2} \tag{9}$$
$$e_{32} = d_{32} - d_{r,3} = X_2 - X_3 - L_3 - d_{r,3} \tag{10}$$
$$e_{31} = d_{31} - d_{r,3} = X_1 - X_3 - L_3 - d_{r,3} \tag{11}$$

are longitudinal spacing errors with $L_i[m]$ being the body length of vehicle i. Let us also define the velocity error $\dot{e}_{ik}$ which is the derivative of e_{ik}:

$$\dot{e}_{ik} = v_k - v_i - ha_i \tag{12}$$

where k is the relevant target vehicle for vehicle i, and a_i is the acceleration of vehicle i in the longitudinal direction. For example, $\dot{e}_{21} = v_1 - v_2 - ha_2$. Therefore, the longitudinal error variable of interest can be determined like (7):

$$e_{x_{ik}} = e_{ik} + c_2\dot{e}_{ik} \tag{13}$$

where $c_2[s]$ is another tuning parameter used to balance these two errors.

3 Controller design

In this section, the Artificial Potential Fields (APF) and corresponding controllers are introduced. Firstly, the theory of artificial potential fields is discussed. Then, functions for both longitudinal and lateral directions are designed. Finally, controllers are proposed for achieving the merging.

3.1 Potential Function Design

The potential function is a real-valued nonnegative function $\Psi_A(e) : \mathbb{R}^m \to \mathbb{R}$, where $e \in \mathbb{R}^m$ is the error state of the system, e.g., lateral error as (7) or longitudinal error as (13). The function Ψ_A can be thought as an artificial energy, which is zero at a desired location, small in desirable regions of the error space and tends to infinity if the error is approaching a restricted region.

To enhance a gap-closing behavior with respect to the preceding vehicle, the potential function (also called Morse-like potential function [9]) is designed as:

$$\Psi_A(e) = k_1(k_3 - e^{-k_2(e-c_e)})^2 \tag{14}$$

where k_1, k_2, k_3 are the parameters to be set, and $c_e = \frac{\ln(k_3)}{k_2}$ so as to make $\Psi_A(0) = 0$. In particular, (14) is re-written to highlight two distinct parts:

$$\Psi_{RP}(e) = \begin{cases} \Psi_A(e), & e<0 \\ 0, & e \geq 0 \end{cases} \tag{15}$$

$$\Psi_{AP}(e) = \begin{cases} \Psi_A(e), & e \geq 0 \\ 0, & e<0 \end{cases} \tag{16}$$

where Ψ_{RP} stands for the repulsive potential part and Ψ_{AP} stands for the attractive potential part.

Fig. 4 shows these two parts of the potential function, which is realized by selecting $k_1 = 0.6, k_2 = 0.04$ and $k_3 = 15.5$. The rationale for the APF is as follows. If e is the longitudinal error, in case $e \ll 0$, a collision is about to happen, therefore the repulsive potential Ψ_{RP} (blue line) increases rapidly as e becomes more negative. It is worth noticing that the gap-closing is enforced by the monotonically increasing Ψ_{AP} (red line): however, when the gap between vehicles becomes too large, gap closing might be not necessary, and $\Psi_{AP}(e)$ converges to a constant for $e \gg 0$. In the next part, we will show how to design control actions along the derivative of the artificial potential fields.

3.2 Lateral and Longitudinal Control

Controllers in the lateral and longitudinal directions are involved in the vehicle merging process, so a potential function for vehicle i can be defined as:

$$\begin{aligned} Z &= \Psi_A(e_{x_{ik}}) + \Psi_A(e_{y_i}) \\ &= k_1(k_3 - e^{-k_2(e_{x_{ik}}-c_e)})^2 + k_1(k_3 - e^{-k_2(e_{y_i}-c_e)})^2 \end{aligned} \tag{17}$$

where $e_{x_{ik}}$ is the error state variable in the longitudinal direction, and e_{y_i} is the error state variable in the lateral direction, as shown in Fig. 5. If vehicle i is on the lane 1, $e_{y_i} = 0$.

Remark 1. In (17), the APF for longitudinal and lateral behavior are taken to be of the same kind, which is done for simplicity of design and to make use of existing design methods. In principle, one can adopt different APF for longitudinal and lateral behavior.
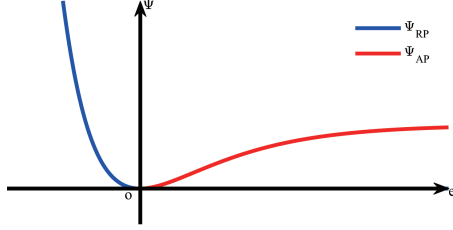
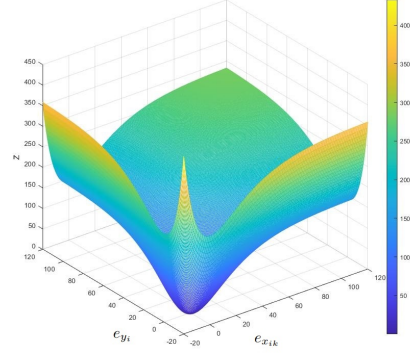**Fig. 4.** The repulsive and attractive Morse-like potential

Fig. 5. The artificial potential function for the two directions

Because the steering angle is relatively small even during merging, the longitudinal and the lateral directions can be controlled separately, which is done in several literature $[1, 5, 16, 24]$. Also, to introduce more realism in the control design, we consider the following actuator dynamics, which represent engine dynamics and steering dynamics (refer to similar approaches in the literature $[5, 10]$):

$$\dot{a}_i = -\frac{1}{\tau_x}a_i + \frac{1}{\tau_x}u_{x_i} \tag{18}$$

$$\dot{\omega}_i = -\frac{1}{\tau_y}\omega_i + \frac{1}{\tau_y}u_{y_i} \tag{19}$$

where $u_{xi}[m/s^2]$ and $u_{yi}[rad/s^2]$ are the inputs to be designed, and $\tau_x, \tau_y[s]$ are the actuator time constants for longitudinal and lateral direction (engine time constant and steering wheel time constant).

The behavior of the merging vehicle in the lateral direction is to make a lane change, so it can treat the adjacent lane as its target which can give an attractive force and treat the previous lane as a obstacle to avoid. Given the lateral part of the potential function (17), the lateral controller which is used to control ω_i can be determined by:

$$u_{y_i} = \frac{\partial \Psi_A(e_{y_i})}{\partial e_{y_i}} \tag{20}$$

During the merging process, in the longitudinal direction, the goal of M_3 is to follow M_2 while a minimum safe distance to M_1 is guaranteed. For M_2, the purpose is to follow M_1. So the control input for M_3 in the longitudinal direction can be determined using the following APF:

$$\Psi_{M_3}(e_{x_{31}}, e_{x_{32}}) = \Psi_{RP}(e_{x_{31}}) + \Psi_A(e_{x_{32}}) \tag{21}$$

To satisfy the requirements of CACC, the ego vehicle should know the control input of its preceding vehicle via wireless communication. Therefore, in line with [10], u_{x_3} which is used to control a_3 can be calculated by:

$$u_{x_3} = \frac{\partial \Psi_{RP}(e_{x_{31}})}{\partial e_{x_{31}}} + \frac{\partial \Psi_A(e_{x_{32}})}{\partial e_{x_{32}}} + u_{x_2}. \tag{22}$$

Similarly, for M_2, if it has a preceding vehicle labeled k on lane 2, the APF can be chosen as $\Psi_{M_2}(e_{x_{2k}}, e_{x_{21}})$ and the control input u_{x_2} which is used to control a_2 is similar to that of M_3:

$$u_{x_2} = \frac{\partial \Psi_{RP}(e_{x_{2k}})}{\partial e_{x_{2k}}} + \frac{\partial \Psi_A(e_{x_{21}})}{\partial e_{x_{21}}} + u_{x_1}. \tag{23}$$

If the merging vehicle is the first vehicle in its previous platoon, which means that M_2 does not have a preceding vehicle k, then the APF is defined as $\Psi_A(e_{x_{21}})$, and u_{x_2} becomes:

$$u_{x_2} = \frac{\partial \Psi_A(e_{x_{21}})}{\partial e_{x_{21}}} + u_{x_1}. \tag{24}$$

The stability of the proposed method relies on the fact that the longitudinal and lateral dynamics can be decoupled, which allows to write $\dot{v}_i = a_i, \dot{\varphi}_i = \omega_i$, i.e. the two inputs affect independently the two directions. The stability analysis of both directions can be done through a Lyapunov approach similar to [9] but is omitted due to the space limitations. We will provide the stability analysis in an extended version of this work.

4   Simulation Results

In this section, simulation results are presented, which are performed in the software CarSim. Three B-class hatchbacks as in Fig. 6 are with geometric parameters listed in Table 1 (engine parameters and other vehicle parameters inside CarSim are consistent with the default parameters of the B-class hatchback and they are not reported for lack of space).

Fig. 6. B-Class hatchback model in CarSim

In the software CarSim, aerodynamics and road friction make the vehicle model more realistic. In addition, CarSim can simulate engine and driveline dynamics that are not included in the control design, thus validating the methodology in a more realistic setting. The CarSim takes the desired longitudinal

acceleration u_{x_i} as an input, and allows to transform the desired lateral acceleration u_{y_i} into the front wheel steering angle δ_f. The related parameters in the controller design are shown in Table 1.

Table 1. Basic Parameters of the Vehicle Model

Parameters	Values
Wheelbase l	2.6 m
Vehicle length L	4.0 m
Time constant τ_x, τ_y	0.06 s
Weight factor c_1	0.3 m/rad
Weight factor c_2	10 s
Standstill distance r_i	5 m
Time gap h	0.5 s

The target speed for the merged platoon is $v = 10\ m/s$. Also, $v_i(0) = 10\ m/s$ for $i = 1, 2, 3$, and the control input $u_{x_1}(0) = 0\ m/s^2$. In the lateral direction, the desired offset $Y_o = -2\ m$ (which represent a lane change) and the desired yaw angle $\varphi_o = 0\ rad$. Two simulations are performed to show the effectiveness of the proposed method.

- In the first scenario, the initial positions of the vehicles are $X_3(0) = 0\ m$, $X_2(0) = 10\ m$ and $X_1(0) = 20\ m$ (large initial gap);
- In the second scenario, the initial positions of the vehicles are $X_3(0) = 0\ m$, $X_2(0) = 5\ m$ and $X_1(0) = 10\ m$ (small initial gap, which requires vehicles M_1 and M_3 to create a sufficiently large gap).

The APF use the same k_1, k_2, k_3 as in Fig. 4. For the first scenario, the simulation results are shown in Fig. 7 and Fig. 8. It is found that at around $t = 32\ s$ the merging process is completed and the platoon has been formed because the longitudinal distance between vehicles like d_{21}, d_{32}, d_{31} is equal to the desired distance $d_{r,i}$; moreover, all vehicles have reached the target speed $v = 10\ m/s$. While in the lateral direction, the merging vehicle M_2 reaches the expected lane change in less than 10 s.

For the second scenario, the simulation results are shown in Fig. 9 and Fig. 10. The initial gaps between vehicles are smaller which are insufficient for vehicle to merge directly, so M_3 needs to create a gap with M_1. In fact, it can be seen that M_3 reaches smaller velocity values than in the first scenario to create the appropriate gap (i.e. it brakes more). The final platoon is achieved at around $t = 38\ s$, which is consistent with the fact that if the initial gap is not large enough, more time will be used to create gap for the merging vehicle.

Fig. 11 collects snapshots of the video produced in CarSim for the first scenario at different times: $t = 0\ s, 5\ s, 15\ s$ and 50 s. The positions of these vehicles corresponds with the above analysis results. Fig. 12 collects snapshots
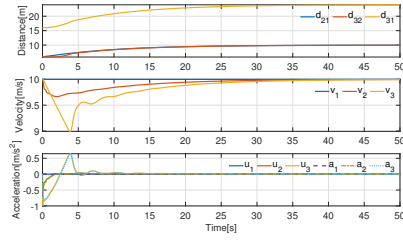
Fig. 7. First scenario (large initial gap): variables in the longitudinal direction
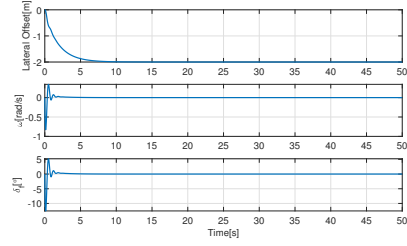

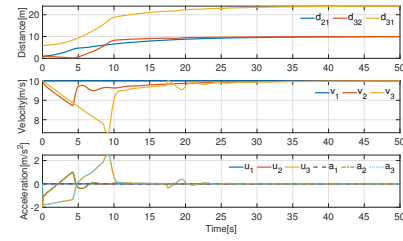**Fig. 8.** First scenario (large initial gap): variables in the lateral direction

Fig. 9. Second scenario (small initial gap): variables in the longitudinal direction
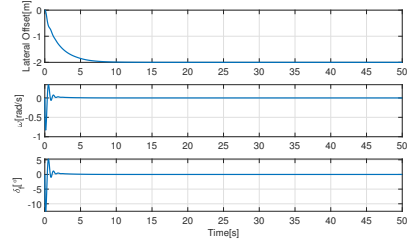

Fig. 10. Second scenario (small initial gap): variables in the lateral direction

of the video produced in CarSim for the second scenario. M_2 and M_3 are very close at time $t = 0\ s$, but it can be seen that M_3 has already created some gap at $t = 5\ s$ to avoid collision. Finally, the desired gap is produced and all control objectives are achieved.

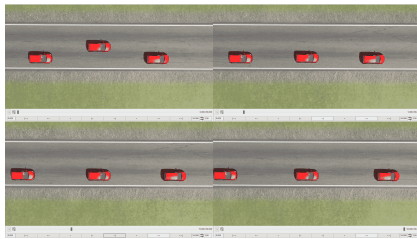**Fig. 11.** Snapshots of vehicles in the first scenario (large initial gap) at times $t = 0\ s, 5\ s, 15\ s$ and $50\ s$.

Fig. 12. Snapshots of vehicles in the second scenario (small initial gap) at times $t = 0\ s, 5\ s, 15\ s$ and $50\ s$.

5 Conclusions

This paper focused on the vehicle merging problem in a cooperative setting (i.e. with gap creating and gap closing features) and proposed longitudinal and lateral control laws using artificial potential fields. In the lateral direction, yaw angle error and lateral offset error were made to converge to zero with the help of the gradient of potential functions. In the longitudinal direction, position error and velocity error were controlled to achieve gap making and gap closing via another potential function. Simulation results in CarSim have shown the effectiveness of the proposed idea. This work is a preliminary study and has used some simplifying assumptions and settings (although motivated from the literature). It is of interest to relax some of these settings in future work, such as: considering variations in the vehicle size, handling explicitly the coupling between longitudinal and lateral dynamics, or handling explicitly curved lines (e.g. by adding a preview distance [25]). Handling the presence of human-driven vehicles is another interesting aspect [26].

References

1. S. A. Hussain, B. Shahian Jahromi, and S. Cetin, "Cooperative highway lane merge of connected vehicles using nonlinear model predictive optimal controller," *Vehicles*, vol. 2, no. 2, pp. 249–266 (2020)
2. A. Schwab and J. Lunze, "Vehicle platooning and cooperative merging," *IFAC-PapersOnLine*, vol. 52, pp. 353–358 (2019)
3. V. Dolk, J. d. Ouden, and S. Steeghs, "Cooperative automated driving for various traffic scenarios: Experimental validation in the gcdc 2016," *IEEE Transactions on Intelligent Transportation Systems*, vol. 19, no. 4, pp. 1308–1321 (2018)
4. T. C. dos Santos, D. R. Bruno, F. S. Osório, and D. F. Wolf, "Evaluation of lane-merging approaches for connected vehicles," in *2019 IEEE Intelligent Vehicles Symposium (IV)*, pp. 1935–1939 (2019)
5. S. Wei, Y. Zou, X. Zhang, and T. Zhang, "An integrated longitudinal and lateral vehicle following control system with radar and vehicle-to-vehicle communication," *IEEE Transactions on Vehicular Technology*, vol. 68, no. 2, pp. 1116–1127 (2019)
6. J. Ploeg, E. Semsar-Kazerooni, and A. I. Morales Medina, "Cooperative automated maneuvering at the 2016 grand cooperative driving challenge," *IEEE Transactions on Intelligent Transportation Systems*, vol. 19, no. 4, pp. 1213–1226 (2018)
7. I. Parra Alonso, D. Izquierdo Gonzalo, and Sotelo, "The experience of drivertive-driverless cooperative vehicle-team in the 2016 gcdc," *IEEE Transactions on Intelligent Transportation Systems*, vol. 19, no. 4, pp. 1322–1334 (2018)
8. M. Karimi, C. Roncoli, C. Alecsandru, and M. Papageorgiou, "Cooperative merging control via trajectory optimization in mixed vehicular traffic," *Transportation Research Part C: Emerging Technologies*, vol. 116, p. 102663 (2020)
9. E. Semsar-Kazerooni, J. Verhaegh, J. Ploeg, and M. Alirezaei, "Cooperative adaptive cruise control: An artificial potential field approach," in *2016 IEEE Intelligent Vehicles Symposium (IV)* (2016)
10. E. Semsar-Kazerooni, K. Elferink, J. Ploeg, and H. Nijmeijer, "Multi-objective platoon maneuvering using artificial potential fields," *IFAC-PapersOnLine*, vol. 50, no. 1, pp. 15 006–15 011 (2017)

11. Y. A. Harfouch, S. Yuan, and S. Baldi, "An adaptive switched control approach to heterogeneous platooning with intervehicle communication losses," *IEEE Transactions on Control of Network Systems*, vol. 5, no. 3, pp. 1434–1444 (2018)

12. S. Baldi, D. Liu, V. Jain, and W. Yu, "Establishing platoons of bidirectional cooperative vehicles with engine limits and uncertain dynamics," *IEEE Transactions on Intelligent Transportation Systems*, pp. 1–13 (2020)

13. S. Baldi, M. R. Rosa, P. Frasca, and E. B. Kosmatopoulos, "Platooning merging maneuvers in the presence of parametric uncertainty," *IFAC-PapersOnLine*, vol. 51, no. 23, pp. 148–153 (2018)

14. D. Liu, S. Baldi, V. Jain, W. Yu, and P. Frasca, "Cyclic communication in adaptive strategies to platooning: the case of synchronized merging," *IEEE Transactions on Intelligent Vehicles*, pp.99: 1–1 (2020)

15. X. Wan, P. J. Jin, F. Yang, and B. Ran, "Merging preparation behavior of drivers: How they choose and approach their merge positions at a congested weaving area," *Journal of Transportation Engineering*, vol. 142, no. 9, p. 05016005 (2016)

16. J. Rios-Torres and A. A. Malikopoulos, "A survey on the coordination of connected and automated vehicles at intersections and merging at highway on-ramps," *IEEE Transactions on Intelligent Transportation Systems*, vol. 18, no. 5, pp. 1066–1077 (2017)

17. M. Hafizulazwan Bin Mohamad Nor and T. Namerikawa, "Merging of connected and automated vehicles at roundabout using model predictive control," in *2018 57th Annual Conference of the Society of Instrument and Control Engineers of Japan (SICE)*, pp. 272–277 (2018)

18. A. Schwab and J. Lunze, "Cooperative vehicle merging with guaranteed collision avoidance," *IFAC-PapersOnLine*, vol. 52, no. 6, pp. 7–12 (2019)

19. A. Schwab, K. Schenk, and J. Lunze, "Networked vehicle merging by cooperative tracking control," *IFAC-PapersOnLine*, vol. 52, no. 20, pp. 19–24 (2019)

20. B. Muller, J. Deutscher, and S. Grodde, "Continuous curvature trajectory design and feedforward control for parking a car," *IEEE Transactions on Control Systems Technology*, vol. 15, no. 3, pp. 541–553 (2007)

21. D. Wang and F. Qi, "Trajectory planning for a four-wheel-steering vehicle," in *Proceedings 2001 ICRA. IEEE International Conference on Robotics and Automation (Cat. No.01CH37164)*, vol. 4, pp. 3320–3325 (2001)

22. H. H. Bengtsson, L. Chen, A. Voronov, and C. Englund, "Interaction protocol for highway platoon merge," in *2015 IEEE 18th International Conference on Intelligent Transportation Systems*, pp. 1971–1976 (2015)

23. V. Jain, D. Liu, and S. Baldi, "Adaptive strategies to platoon merging with vehicle engine uncertainty," *IFAC-PapersOnLine*, vol. 53, no. 2, pp. 15 065–15 070 (2020)

24. R. Kianfar, M. Ali, P. Falcone, and J. Fredriksson, "Combined longitudinal and lateral control design for string stable vehicle platooning within a designated lane," in *17th International IEEE Conference on Intelligent Transportation Systems (ITSC)* (2014)

25. A. Morales and H. Nijmeijer, "Merging Strategy for Vehicles by Applying Cooperative Tracking Control," *IEEE Transactions on Intelligent Transportation Systems*, vol. 17, no. 12, pp. 3423-3433 (2016)

26. V. Giammarino, S. Baldi, P. Frasca and M. L. D. Monache, "Traffic Flow on a Ring With a Single Autonomous Vehicle: An Interconnected Stability Perspective," *IEEE Transactions on Intelligent Transportation Systems*, vol. 22, no. 8, pp. 4998-5008 (2021)